THE JOURNAL OF PHYSICAL CHEMISTRY C

Article

pubs.acs.org/JPCC

Effect of Molecule–Surface Reaction Mechanism on the Electronic Characteristics and Photovoltaic Performance of Molecularly Modified Si

Omer Yaffe,[†] Tal Ely,[†] Rotem Har-Lavan,[†] David A. Egger,[‡] Steve Johnston,[§] Hagai Cohen,[∥] Leeor Kronik,*[,†] Ayelet Vilan,*[,†] and David Cahen*[,†]

[†]Department of Materials & Interfaces, Weizmann Institute of Science, Rehovoth 76100, Israel

[‡]Institute of Solid State Physics, Graz University of Technology, A-8010 Graz, Austria

[§]National Renewable Energy Laboratory, Golden, Colorado 80401, United States

[∥]Department of Chemical Research Support, Weizmann Institute of Science, Rehovoth 76100, Israel

Supporting Information

ABSTRACT: We report on the passivation properties of molecularly modified, oxide-free Si(111) surfaces. The reaction of 1-alcohol with the H-passivated Si(111) surface can follow two possible paths, nucleophilic substitution (S_N) and radical chain reaction (RCR), depending on adsorption conditions. Moderate heating leads to the S_N reaction, whereas with UV irradiation RCR dominates, with S_N as a secondary path. We show that the site-sensitive S_N reaction leads to better electrical passivation, as indicated by smaller surface band bending and a longer lifetime of minority carriers. However, the surface-insensitive RCR reaction leads to more dense monolayers and, therefore, to much better chemical stability, with lasting protection of the Si surface against oxidation. Thus, our study reveals an inherent dissonance between electrical and chemical passivation. Alkoxy monolayers, formed under UV irradiation, benefit, though, from both chemical and electronic passivation because under these conditions both S_N and RCR occur. This is reflected in longer minority carrier lifetimes, lower reverse currents in the dark, and improved photovoltaic performance, over what is obtained if only one of the mechanisms operates. *These results show how chemical kinetics and reaction paths impact electronic properties at the device level.* It further suggests an approach for effective passivation of other semiconductors.

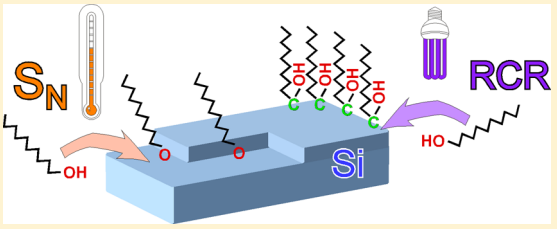

INTRODUCTION

Organic monolayers (MLs) on oxide-free Si surfaces[1] have been studied extensively as a viable and effective tool to control the electronic properties of Si (see ref 2 and references therein). The basic idea that lies at the heart of these studies is that by combining molecular functionality with the robustness of Si technology we can create hybrid (organic–Si) systems that will extend and improve the possibilities of existing devices and provide options for new ones. To date, the chemical ability to control interfacial electrical properties of semiconductor junctions, via molecule–surface interactions and by way of pure molecular properties, is one of the more powerful manifestations of molecular effects on electronic devices.[2] Furthermore, such hybrid systems are very useful in the more general study of fundamental properties of semiconductor interfaces due to the large variety of molecules that can be bound to the surface through the various binding configurations that allow controllable surface modification.[2] Adsorbing a molecular monolayer onto a semiconductor contributes to three aspects of the semiconductor surface, which are critical for optimizing device performance:

a. Control over the effective work function (WF), i.e., the semiconductor surface potential, via a surface molecular dipole layer (cf., e.g., refs 3–10) to tune the energetics of the interfaces, formed with this semiconductor surface;

b. Electronic passivation of the Si surface, to reduce the density of surface states,[11−14] which cause high leakage currents in diodes and poor performance in solar cells[15,16] and, in general, limit the efficacy of translating WF modification (**a**, above) into interface tuning. Chemical binding removes dangling bonds and/or surface reconstruction or stresses at defects, thereby eliminating surface states.

c. Formation of strong chemical bonds to undercoordinated surface atoms. Because native oxidation is incomplete, it introduces electrical states and traps which degrade electrical performance. Strong chemical bonding considerably reduces the reactivity of these states and, therefore, provides chemical

Special Issue: Ron Naaman Festschrift

Received: March 20, 2013
Revised: May 27, 2013
Published: June 3, 2013

passivation of the semiconductor surface, mostly to prevent surface oxidation over time and under extreme conditions.[17−20]

The above considerations apply in principle to any semiconductor, but here and throughout we naturally emphasize Si as its unique place in modern technology and its widely studied surface chemistry make it a highly desired candidate for the study of molecular treatments.

A major challenge for future practical use of organic molecules for Si passivation is that all of the above-mentioned demands, namely, control over the WF, electronic passivation, and chemical passivation, must be fulfilled by one and the same molecular monolayer. To meet this challenge, a fundamental understanding of how molecules are bound to the Si surface and of the effect of each binding configuration must be gained. In the present study, we show that the requirements for a monolayer that provides efficient electronic passivation are not similar and can even be contradictory to the requirements for efficient chemical passivation. On the basis of experimental results and organic reaction mechanisms we suggest chemical insight that relates between chemical reactivity and the efficiency of electrical passivation. In addition, we demonstrate and provide guidelines for monolayer preparation that provides both chemical and electronic passivation. Together with previous studies that demonstrated control over the WF of the Si surface, these results provide a viable route toward implementation of molecular electronics in electronic devices, including photovoltaic (PV) cells.

Background and Approach. The nature of the chemical bond between the molecules and the substrate is known to be an important factor for the quality of a monolayer, formed with these molecules, and, in the case of a semiconductor substrate, in determining the electronic properties of the modified surface.[3,22,23] Commonly, the effect of molecular anchoring is studied by using different precursor binding groups for forming the monolayer.[7,24,25]

However, a given molecule can react via more than one mechanism, leading to more than one product. Such is the case for monolayer formation from alkyl alcohols on Si(111), as we shall illustrate here by way of the reaction of a primary alcohol (decanol) with the H-terminated Si surface. According to traditional solution chemistry, this reaction can proceed via two different mechanisms:

a. nucleophilic substitution (S_N) of an alkoxide (conjugated base of the alcohol) that proceeds (for the ideal Si(111) surface) through a pentavalent silicon complex as an intermediate species[21,26] (Figure 1a);
b. radical chain reaction (RCR) where a radical is created on the Si surface, which initiates a chain reaction that binds molecules to the surface and propagates until the radical is eliminated (Figure 1b).[27]

There are three notable differences between these two reaction mechanisms. The first one concerns the reaction product. The binding configuration of the S_N reaction product is expected to be Si−O−CH_2−R (R = $C_8H_{16}CH_3$, Figure 1a).[19,26,28] The expected binding configuration in the RCR product is different. From solution chemistry it is expected that the free radical, created on the Si surface, will attack and remove a H atom from the α-carbon (the carbon attached to the OH group),[29−32] leading to the Si−CH(OH)−R binding configuration (Figure 1b). This binding configuration was not considered for monolayers before. Between the two, above-described, binding configurations the latter (Si−CH(OH)−R)

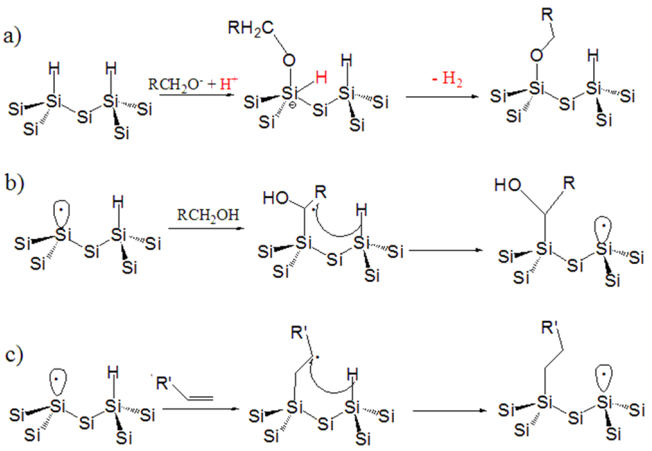

Figure 1. Simplified schemes of the different reaction mechanisms on Si(111) and resulting monolayer structures. (a) Reaction of 1-aloxide (conjugated base of 1-alcohol[21]) via S_N mechanism, as a result of moderate heating to 80 °C. (b) Reaction of 1-alcohol via RCR mechanism, initiated by UV irradiation. (c) Reaction of 1-alkene via RCR mechanism initiated by high thermal activation (200 °C). R = $C_8H_{16}CH_3$; R′ = $C_9H_{18}CH_3$.

is expected to be more stable than the former (Si−O−CH_2−R). This is because the more polarized Si−O bond (due to the high electronegativity of the O atom) is more susceptible toward hydrolysis than the less polar Si−C bond.[11,33,34]

The second important difference is that the S_N reaction of alcohols with Si−H is site-sensitive, while the RCR is not. The H−Si(111) surface is known to be a close to ideal, Si-monohydride-terminated, atomically flat one.[35,36] However, a Raman spectroscopy study showed different sites on such a Si surface, such as kinks, dihydride edge sites, monohydride edge sites, and terrace sites that all have different chemical reactivity toward an etching solution.[37] The different Si surface sites exhibit also different reactivity toward the S_N reaction with an alcohol, and the reaction rate for the more reactive sites (e.g., kinks) is orders of magnitude larger than that for the less reactive sites (e.g., the terrace site). Therefore, on the more reactive sites the reaction takes place immediately, even at room temperature.[21] In RCR, the radical is generated randomly on the Si surface and initiates the formation of a close-packed monolayer in its vicinity.[38]

The third difference is in the monolayer growth dynamics. RCR proceeds through the migration of the free radical from one Si surface atom to the next. Thus, the monolayer growth is found to proceed via formation of irregularly shaped, dense islands that appear to grow by a pseudorandom walk process.[39] Furthermore the monolayer growth is rapid.[27] The high rate and island-like growth are beneficial for preparation of very dense monolayers because of relatively minor steric effects, which prevent additional molecules from reaching the surface. Contrary to the RCR, the S_N reaction is rapid only for the most reactive sites and much slower for the majority of the surface Si atoms (terrace sites). Furthermore, the formation of the monolayer is scattered rather than via densely packed islands. Such scattered binding leads to a less dense monolayer because already at moderate binding density steric hindrance limits the availability of free adsorbates. Therefore, we expect an S_N made monolayer to be less dense than the monolayer formed via RCR.

We expect for the binding configuration and more so the reaction kinetics and monolayer growth to have a marked effect

dx.doi.org/10.1021/jp4027755 | J. Phys. Chem. C 2013, 117, 22351−22361

on the passivation properties of the final layer. [Note: We expect that the binding configuration will also have an effect on the molecule−substrate electronic coupling, as demonstrated elsewhere (see refs 26 and 73). The proper study of electronic coupling requires the use of degenerate Si substrates and is beyond the scope of this work.]

To explore it, we choose reaction conditions, which are known to give preference to specific reaction routes:

a. 12 h of moderate heating of the 1-alcohol melt (80 °C), which is high enough to increase the S_N reaction rate but not sufficiently high to initiate the formation of radicals on the Si surface.[40] Therefore, monolayer formation would proceed predominantly via the S_N mechanism. This is denoted as "alkoxy$_{80}$".

b. 3 h of UV irradiation at room temperature (denoted as "alkoxy$_{UV}$"), where radicals are created by the UV light and most of the monolayer is formed via RCR. Still, defect sites on the Si surface would be sufficiently reactive to induce a S_N reaction even at room temperature. Hence, the alkoxy$_{UV}$ monolayer represents a mixed RCR and S_N case, with a dominant RCR portion.

A pure RCR monolayer is realized by a third type of monolayer made of 1-alkene (1-dodecene) by 3 h of thermal activation at 200 °C (denoted as "alkyl"). The alkyl monolayer is known to form a highly dense monolayer (~50% coverage with respect to the total Si surface atoms) with reproducible electronic transport properties.[41−45] Contrary to the 1-alcohol, where two reaction mechanisms are possible, the alkyl monolayer can be formed only via RCR (Figure 1 c), regardless of initiation by heat (>150 °C),[40] UV light, or addition of peroxides.[41] The conditions used here were shown to produce highly reproducible alkyl monolayers.[43]

In this study we combine organic, physical, theoretical, surface, inorganic, and materials chemistry to elucidate the role of adsorbate binding chemistry on the electrical properties of Si surface and interface. We show that indeed the different reaction conditions (i.e., heating and UV irradiation) lead to monolayers that are of similar stoichiometry but profoundly different in terms of the chemical and electronic passivation, as well as the effective work function of the resulting surface. This clear observation can only be rationalized by different binding configurations. While resolving a definite chemical structure for stoichiometrically close, ~1 nm thick, disordered monolayers is beyond present capabilities, we rely on a novel combination of spectroscopic, electrostatic, and computational tools to offer evidence in favor of the different binding configuration of Figure 1. Furthermore, by using mercury as a top contact we show the effects of differences in electronic passivation and bond dipole on the current−voltage characteristics of the Hg/molecules/Si junctions, in the dark and under illumination, i.e., their diode and photovoltaic performance.

EXPERIMENTAL AND COMPUTATIONAL DETAILS

Sample Preparation. Wafers of n-type Si with (111) orientation were purchased from Virginia Semiconductors (USA), with two different doping levels, required for different characterization methods. Photoconductive decay (PCD) measurements were performed on double side polished, float zone (FZ) grown Si with nominal resistivity of 1800−2500 Ω·cm. All other measurements were performed on single side polished n-type Si(111) wafers with a nominal resistivity of 1−10 Ω·cm.

Alkyl and alkoxy$_{80}$ sample preparation followed literature descriptions.[25,43] Briefly, ~1 × 1.5 cm^2 pieces were cleaned by sequential rinsing with ethyl acetate, acetone, ethanol, and doubly distilled water (DDW) and then immersed in piranha solution, i.e., 3:7 by volume of 30% H_2O_2 and H_2SO_4, (**caution: strong oxidizing solution, handle with care**) for 30 min, followed by etching for 10 min in 40% (v/v) NH_4F solution in water, which was previously degassed with a N_2 flow for 30 min. The piranha and NH_4F steps were repeated twice, and the resulting H-terminated Si was rinsed with DDW, N_2 dried, and immediately immersed (using a Schlenk line) in neat liquid, oxygen-free 1-dodecene and 1-decanol at 200 and 80 °C, respectively. The preparation of alkoxy$_{UV}$ followed the same procedure for receiving a clean, hydrogen-terminated Si, which was then immersed in 1-decanol at room temperature in a quartz vial. The vial was illuminated for 2.5 h with UV irradiation of 254 nm in a glovebox (~0.1 ppm O_2). After adsorption, all molecularly modified Si samples were sonicated in acetonitrile for 3 min, rinsed with boiling dichloromethane, and dried over a N_2 flow. Modified Si samples were usually characterized immediately after preparation, except in the case of PCD measurements (performed at NREL, USA), in which case they were stored for 7 days in a N_2-filled tube after preparation.

Sample Characterization. Molecularly modified samples were characterized by ellipsometry (M 2000 V, J.A. Woollam) and Fourier transform infrared (FTIR) spectroscopy (Thermo-Nicolet, 6700), using a Ge attenuated total reflection accessory (HARRICK VariGATR) and H-terminated Si as reference; X-ray photoelectron spectra (XPS, Kratos AXIS ULTRA) were employed, with a monochromatic Al Kα X-ray source at 75 W, detection pass energies ranging between 20 and 80 eV, and peak decomposition by CasaXPS, using linear background and a peak shape of Gaussian/Lorentzian product (30% Lorentzian). To avoid too many peaks, an exponential tail was added to the main C 1s component.

Contact Potential Difference (CPD). Measurements were performed with a homemade Kelvin probe setup, based on a commercial Besocke Delta Phi Kelvin probe and controller, placed in a controlled atmosphere box with 10% relative humidity. The surface potential of the monolayers was measured, relative to that of a vibrating Au grid, which was calibrated prior to the measurements against freshly peeled highly ordered pyrolytic graphite (HOPG).

Photoconductivity Decay (PCD). Lifetime measurements were performed with a radio frequency photoconductivity decay (RF-PCD) measurement technique, operating in the ultrahigh frequency (UHF) range of 700 MHz.[46] The minority-carrier injection source was an attenuated 1064 nm YAG laser with a spot size of approximately 5 mm.

Current−Voltage. Current−voltage measurements were performed on n-Si/monolayer/Hg junctions, formed by placing a Hg (99.9999% purity) drop on the monolayer, using a mercury drop electrode (Polish Academy of Sciences, Poland). The samples were contacted at the back by applying an In−Ga eutectic, after scratching the surface with a diamond knife. Measurements were carried out in a controlled environment glovebox with 10% relative humidity. The contact area between the Hg drop and the monolayer (typically 0.6 mm in diameter) was determined using an optical microscope. The current/voltage source-measure unit was a Keithley 6430 sub-fA.

Electronic Structure Calculations. The Si surface was represented by a 12 layer Si(111) slab in a (2 × 1) surface unit

cell. The surface coverage was chosen to be 50%; i.e., half of the surface Si atoms are bound to an alkyl chain, and the remaining dangling Si bonds are saturated with hydrogen. This choice was made because it is known to be experimentally correct for alkyl (ethyl and higher) monolayers.[41−45] For the alkoxy monolayer, detailed coverage data are not known. However, the data in Table 1 strongly suggest that the coverage is similar for the alkyl and the alkoxy monolayers. It was previously shown that the electronic structure of alkyl chains, as well as its effect on the work function, saturates after the fourth carbon from the Si surface.[47] Therefore, here each alkyl or alkoxy chain was modeled computationally by 6 carbons, even though 10−12 carbons were used in the experiment. This allowed us to reduce the computational cost without compromising the predictive power for the electronic structure.

Table 1. Static Water Contact Angle (SWCA), Ellipsometric Thickness, and IR ν_a (CH_2)[a]

	SWCA [°]	d [Å]	$\nu_a(CH_2)$ [cm^{-1}]
$alkoxy_{80}$	106 ± 3	16 ± 1	2923
$alkoxy_{UV}$	108 ± 2	16 ± 1	2920
alkyl	110 ± 2	17 ± 1	2918−2920[b]

[a]Errors are the standard deviation between at least 10 separately prepared samples. [b]Taken from ref 43 and similar to ref 17.

We also note that the monolayers are known to be disordered,[48] while the computational model is for an ordered monolayer. Therefore, the use of DFT in this study is only to explore how the electronic properties (work function, core level shifts) depend on the assumed structure, rather than to reproduce experimental results.

Density functional theory (DFT) computations were performed using the Perdew−Burke−Ernzerhof (PBE) generalized-gradient approximation functional[49] as implemented in the Vienna ab initio simulation package (VASP) plan wave code.[50] We employed an (11 × 11 × 1) Monkhorst−Pack k-point sampling and 400 eV energy cutoff. Unless otherwise noted, a symmetric slab configuration was used to prevent a net dipole, perpendicular to the surface.[51−53] The atoms in the unit cell were relaxed until all ionic forces were below 0.01 eV/Å. Similar simulation parameters were found to be sufficient for convergence of the electronic structure in previous studies of the Si surface, e.g., refs 9 and 47.

XPS simulations were performed by calculating the energy difference upon exciting the C 1s core levels of the bonding carbon and the fourth carbon (middle of the chain) in each alkyl chain (cf. Figure 1). We employed the final-state approximation, as implemented in the VASP code,[54] and used an asymmetric-slab configuration together with a dipole correction,[51] applied perpendicular to the surface.

Changes in the surface dipole were computed by considering the averaged electrostatic potential, perpendicular to the surface,[52] calculating the energy differences between the vacuum region and a local maximum point, found in the middle of the slab for each of the systems, and comparing this to the pristine H-terminated Si surface.[9,55]

RESULTS AND DISCUSSION

Structural and Chemical Characterization. Ellipsometry and static water contact angle (SWCA) were measured for every sample prior to electronic characterization of the samples. Average values are summarized in Table 1. These values are similar to those of previous reports and indicate that the ML formation was successful.[25,43] The SWCA of the $alkoxy_{80}$ (dominated by S_N) samples is slightly lower than that of the RCR dominated samples ($alkoxy_{uv}$ and alkyl), but only within the margin of error. However, the position of the antisymmetric methylene stretching vibration, $\nu_a(CH_2)$ in the IR spectrum, which is commonly used as an indicator of the intermolecular environment of alkyl chains,[56−58] indicates that the $alkoxy_{80}$ monolayer is indeed less dense than the RCR dominated monolayers. As mentioned in the previous section (Background and Approach), this is expected.

To further characterize the resulting monolayers, we used FT-IR measurements to detect the presence of oxygen in the alkoxy monolayers. Both the Si−O−R and C−O stretching frequencies are typically around 1100 cm^{-1}.[59] As shown in Figure 2, the alkyl control sample does not exhibit a signal around this frequency, whereas such a signal is clearly observed for both alkoxy samples. There are no frequencies, corresponding to Si−O−CH_2−R bonds in the alkyl monolayer, while they do appear for both the $alkoxy_{80}$ and $alkoxy_{UV}$ samples.

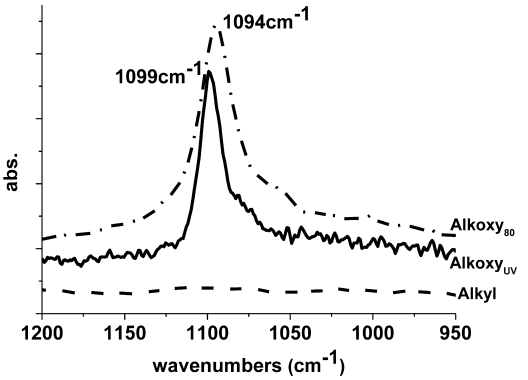

Figure 2. FT-IR spectra of the Si−O−CH_2−R alkoxide region for Si-$alkoxy_{80}$ (dash-dot), Si-$alkoxy_{UV}$ (solid), and Si-alkyl (dash) monolayers. A peak at ∼1100 cm^{-1} is clearly visible for both alkoxy monolayers but absent for the alkyl monolayer.

FT-IR is also expected to show the presence of the OH group (∼3300 cm^{-1})[59] in the $alkoxy_{UV}$ sample. Indeed as indicated in Figure S1 in the Supporting Information, a clear and typical OH stretch is observed in the $alkoxy_{UV}$ monolayer. However, similar peaks were also observed for some of the alkyl monolayers, where such a peak is not expected. This is because, unfortunately, there are multiple sources for OH, such as residues of OH groups directly bound to the Si surface,[33] and, notwithstanding strict humidity control, miniscule fluctuations of humidity and therefore varying amount of OH groups (e.g., from physisorbed water) on the spectrometer optics. This is the reason that the OH mode is rarely reported in the literature on monolayers prepared by solution chemistry (and in the few cases that it is, it was not found to be very informative[60]). Thus, it cannot really serve as a useful indicator for monolayer binding configuration, without careful isotopic exchange studies or in situ UHV reaction studies.[61]

Further indication of the binding configuration is obtained from high-resolution XPS scans of the C 1s emission peaks (Figure 3). The data are presented with decomposition into synthetic components. The energy scale was shifted to lower binding energy (BE) by 0.17−0.45 eV (varies between different samples), to bring the main C 1s peak component to 285.0 eV, i.e., to correct for possible band bending in the Si and/or for

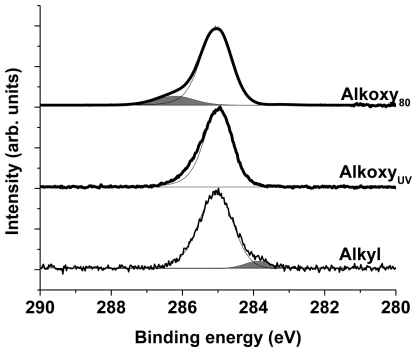

Figure 3. XPS C 1s spectral region for the three types of monolayers (see tags) decomposed into a primary (assigned to CH_2) and secondary peak (gray) which is assigned to the alkyl chain carbon that is closest to the Si surface. The BE scale was shifted to align the center of the C 1s peak at 285 eV.

other surface charging effects. The main C 1s peak is the neutral C peak, as in CH_2, and is similar for all samples. However, the secondary component of each C 1s peak (gray) is clearly different for the different samples. This provides a sensitive indication for a different binding configuration in the three monolayers. For the alkyl, the secondary component is shifted to a lower BE by −1.4 eV. This is typical for carbon bound to a Si atom (C−Si).[62] Since the electronegativity of Si is less than that of C, the carbon bound to the Si surface is more negatively charged (i.e., reduced, with a lower C 1s BE) than the rest of the carbons in the alkyl chain. The secondary C 1s component of the $alkoxy_{80}$ is shifted from the main peak by 1.2 eV to higher BE (i.e., oxidized), as expected for C, bound to O.[25]

Contrary to the other two samples, for the $alkoxy_{UV}$ sample the secondary C 1s component is not typical. It is not well resolved from the main peak, and several different decompositions gave similarly good fits. The fact that the secondary peak is not well resolved can be explained as follows: the carbon that is bound both to Si (reducing) and to oxygen (oxidizing) is expected to have a binding energy, influenced by these two opposite effects, and its BE shift is expected to be intermediate between that of C−Si (as in alkyl) and that of C−O (as in $alkoxy_{80}$).

To test this hypothesis, we performed a DFT computation (see methods) to obtain typical trends in the electronic structure of all three relevant Si-monolayer structures (see Figure 1, right column of a, b, and c). Then, we computed the shifts in C 1s binding energy of the first carbon in each structure, compared to the C atom in the middle of the alkyl chain. The computed BE shifts were: −1.1 eV for C−Si (Figure 1c), +1 eV for C−O (Figure 1a), and > 1.0 eV for Si−CH(OH)−R (Figure 1b). The first two computed BE shifts are in excellent agreement with the experimental results of Figure 3 for alkyl and $alkoxy_{80}$, respectively. The calculation for the Si−CH(OH)−R configuration (Figure 1b) shows that the shift in C 1s of a carbon, bound to both Si and O, should be close to null. This computational result indeed supports our hypothesis that the $alkoxy_{UV}$ monolayer has a binding configuration of Si−CH(OH)−R as shown in Figure 1b. Nevertheless, our results would also be consistent with a small fraction of the $alkoxy_{UV}$ in a binding configuration of $Si-O-CH_2-R$ (Figure 1a), owing to room-temperature nucleophilic substitution at highly reactive sites. In fact, the electronic properties that are presented in the following suggest that such concurrent nucleophilic substitution does occur.

Chemical Passivation. The quality of the monolayer can be judged from the amount of residual oxidized Si, which can easily dominate the electrical properties of organic monolayer−Si systems.[43]

Figure 4 shows the Si 2p peak, where we plot the log of the intensity to increase our sensitivity to a signal in the 103−104 eV BE region where that of Si bound to oxygen is expected. The absence of such a signal provides a first indication for the efficient chemical passivation of the Si surface by each of the three monolayers.

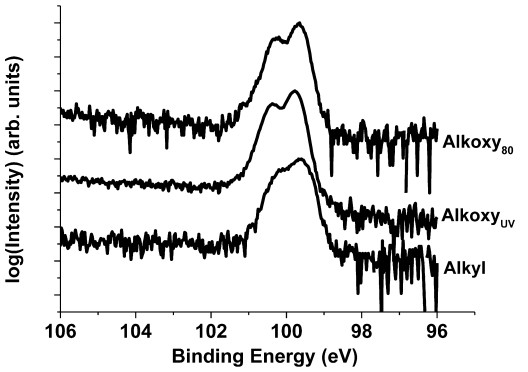

Figure 4. High-resolution XPS for the Si 2p region of the Si substrate under three types of alkyl monolayers (see tags). Spectra are plotted on a semilogarithmic scale to emphasize the absence of residual SiO_2 by the lack of signal in the 103−104 eV binding energy region.

Although the XPS data (Figure 4) showed no difference between the three types of monolayers in terms of immediate oxidation, the more important question is the long-term chemical passivation, namely, the degree to which the different monolayers protect the Si surface against the formation of native SiO_2. We used 1 h immersion in boiling water, which we assume to accelerate the formation of SiO_2,[63] and current−voltage measurements, known to be very sensitive to minute amounts of oxides.[43] Figure 5 presents the current−voltage behavior of the Si-$alkoxy_{80}$/Hg (Figure 5a) and Si-$alkoxy_{UV}$/Hg junctions (Figure 5b), before (solid line) and after (dashed line) a 1 h exposure to boiling water. The results for the Si-alkyl/Hg junction are similar to those of the Si-$alkoxy_{UV}$ (not shown).

Clearly, the $alkoxy_{80}$/Hg junction is strongly affected by exposure to water, while the Si-$alkoxy_{UV}$/Hg one is only slightly affected. This agrees with previous reports where alkoxy monolayers, prepared by moderate heating to 80 °C on oxide-free Si, were reported to be less stable than alkyl monolayers on Si.[19,64] Two factors contribute to the improved chemical passivation of the $alkoxy_{UV}$ compared to the $alkoxy_{80}$ monolayer. The first is the somewhat higher density of the $alkoxy_{UV}$ monolayer, inferred from the FTIR data of Table 1. The second is the difference in binding configuration of the monolayers. The higher electronegativity of O than of C makes the Si atom, to which the O binds, more oxidized (positive) than a Si surface atom bound to C. The O-bound Si ($alkoxy_{80}$) is, therefore, more susceptible to nucleophilic substitution than the C-bound one ($alkoxy_{UV}$).[40,64]

In summary, chemical characterization suggests that all three monolayers are of high quality (CA ≥ 106°, $\nu_a(CH_2) \leq 2923$ cm^{-1}) with the $alkoxy_{80}$ monolayer being slightly less dense

dx.doi.org/10.1021/jp4027755 | J. Phys. Chem. C 2013, 117, 22351−22361

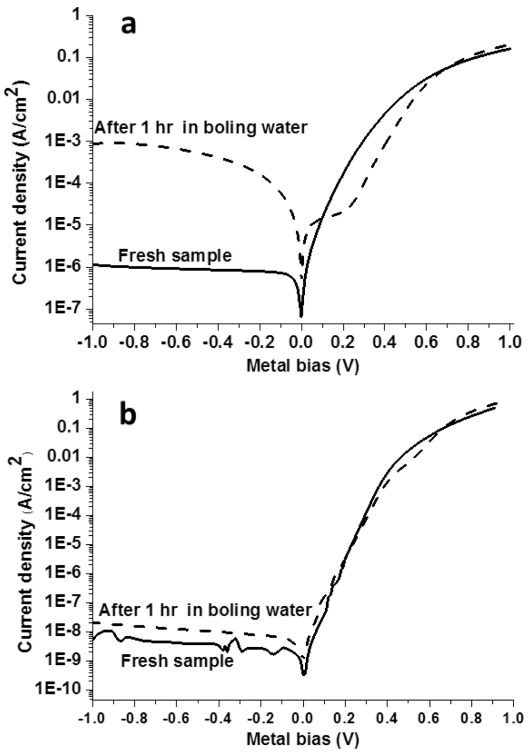

Figure 5. Current density–voltage behavior of (a) the Si-alkoxy$_{80}$/Hg and (b) Si-alkoxy$_{UV}$/Hg junction, before (solid line) and after (dashed line) a 1 h exposure to boiling water.

than the alkoxy$_{UV}$ one, which, in turn, is slightly less dense than the alkyl monolayer (see Table 1). This is expected in light of the differences in growth dynamic of the different chemical mechanisms as discussed in the background section. No oxidized Si can be detected on any of the three fresh monolayers (Figure 4), though aging was much faster for the alkoxy$_{80}$ than for the alkoxy$_{UV}$ monolayer (Figure 5). On the basis of IR (Figure 2), the C 1s XPS emission peak (Figure 3), and DFT computations we deduce that while the alkyl and alkoxy$_{80}$ monolayers have homogeneous binding configurations of Si–CH$_2$–R and Si–O–CH$_2$–R, respectively, the alkoxy$_{UV}$ monolayer has a binding configuration of Si–CH(OH)–R, with possibly a small amount of molecules bound in a Si–O–CH$_2$–R configuration at the most reactive sites of the Si surface (e.g., kinks and steps[21]). This is further discussed after the presentation of the electronic passivation measurements.

Next, we turn to the study of the electronic properties of the different samples.

Electronic Characterization. *Surface Potential and Surface Dipole.* The two key roles of organic monolayers in modifying the electronic properties of the Si surface are reduction of the density of surface states (electronic passivation) and introduction of a surface dipole.[65] To a first approximation, the surface dipole, associated with a molecular monolayer that is chemisorbed on a solid surface, is considered to be composed of the molecular dipole and the surface–molecule bond dipole and to be affected by the molecular coverage.[9,66−68] The change in surface potential (or WF), induced by the molecular modification, can be approximately measured as the difference between the measured photo-saturated CPD value, CPD$_L$ (i.e., under strong illumination) in the molecularly modified sample, and a given reference sample.[69,70] In this study the reference sample is the hydrogen passivated Si(111) surface. Those differences, which we interpret as changes in surface dipole, are given in Table 2—first column. Electronic passivation is quantified by two methods: First, by measuring the difference between CPD$_L$ and the CPD value of the same sample in the dark (CPD$_D$), which is taken as a measure of the band bending (BB) at the molecularly modified Si surface (Table 2—second column). Second, by measuring the photocurrent decay time, from which we calculate the effective minority carrier lifetime (τ_{eff}) of the different samples (Table 2—third column).

Table 2. Change in Electron Affinity (ΔCPD$_L$), Measured Si Band Bending (CPD$_L$–CPD$_D$), and Minority Carrier Lifetime (τ_{eff}) of Monolayer-Modified Si Surfaces[a]

	ΔCPD$_L$ wrt Si–H [meV]	CPD$_L$–CPD$_D$ [meV]	τ_{eff} [μS]
alkoxy$_{80}$	−330 ± 15	55 ± 15	N/M[b]
alkoxy$_{UV}$	−690 ± 20	100 ± 35	200 ± 50
alkyl	−450 ± 22	240 ± 40	50 ± 20

[a]Errors are standard deviation between different measurements. [b]Due to lack of stability over time.

The reduction of the Si:H surface dipole by the alkyl monolayer, found in Table 2 to be ∼0.45 eV, is consistent with other reports and has been rationalized previously.[62,71] The surprising aspect, however, is the ∼0.35 eV difference in the surface dipole of the alkoxy$_{80}$ and alkoxy$_{UV}$ modified surfaces. While the density of the alkoxy$_{UV}$ monolayer is indeed somewhat larger, this modest difference cannot explain the magnitude of the observed change in surface dipole. However, this strong variation in surface dipole is fully consistent with the different binding configurations of the different monolayers, as emerging from the chemical characterization above. The alkoxy$_{80}$ monolayer is only Si–O bound. Because O has a higher electronegativity than C, this type of bonding is expected to increase the WF, compared to that of the completely Si–C bound alkyl monolayer. Indeed, the experimental results indicate that the WF of alkoxy$_{80}$ is higher than that of the Si-alkyl sample. However, the alkoxy$_{UV}$ monolayer also has molecules bound via the α-carbon (see Figure 1b). This binding configuration is expected to strongly affect the dipole at the Si–molecule interface due to the presence of the polar OH group.

To further understand the microscopic origins of the observed change in surface potential, we performed DFT computations for the work function, associated with the three binding configurations of Figure 1, as well as for the H-passivated Si(111) surface, serving as our reference. This yielded surface dipole variations of −700 and −500 meV with the models used above (Figure 1) for the alkyl and alkoxy$_{80}$ monolayers, respectively. This result is in good agreement with the experimental data, especially if we consider also the disorder in the actual monolayers. For the model alkoxy$_{UV}$ monolayer, the situation is complicated by a strong dependence of the computed surface dipole on the orientation of the OH group with respect to the Si surface. To illustrate this, we computed the surface dipole for two extreme orientations of the OH—with torsion angles between the Si surface and the H atom of 180° and 0° (with no further geometrical optimization). This simple C–O bond rotation resulted in a work function change of −1300 and +400 meV, respectively, i.e., spanned a large work function range of ∼1.7 eV. This remarkably large effect is due solely to the polarity of the O–H bond. A comparison to

the experimental result indicates that the surface dipole of the alkoxy$_{UV}$ monolayer is negative and very large. Therefore, we infer that the equilibrium torsion angle in the sample is closer to 180° than to 0°.

Electronic Passivation of the Si Surface. While the alkyl monolayer seems to be the most dense and hydrophobic one (Table 1), the band bending (BB) and minority carrier lifetime (τ_{eff}) values indicate that the alkoxy (both thermal and UV) monolayers are more effective in electrically passivating the Si surface than the alkyl monolayer. We explain this result by recalling that specific sites on the Si surface, such as kinks and steps, which are responsible for surface states,[72,73] are also highly reactive toward alcohol molecules. Once the freshly etched Si surface is in the alcohol solution, even at room temperature (e.g., for photoactivated alkoxy$_{UV}$), the alcohol molecules bind via S_N selectively to the more reactive sites and by that passivate a major part of the surface states. Contrary to this, the alkyl monolayer forms only via RCR (as S_N is impossible), and therefore, the molecules have no preference toward reactive defect sites. As a result, the surface state passivation is not efficient. This explains our finding that the alkoxy monolayer is superior for electronic passivation of the oxide-free Si(111) surface.

Thus, we observe an inherent tension between chemical passivation, which requires a bond with small polarity such as the Si−C bond that forms only via RCR mechanism and is not susceptible toward hydrolysis, and electronic passivation that is provided through the site-sensitive S_N reaction but results in the more polar but, therefore, relatively unstable Si−O bond. This conflict, i.e., the contradicting demands for chemical and electronic passivation, is not usually considered. The reason for that is that the outcome of poor chemical passivation—native SiOx—is directly connected to poor electronic passivation by (nonstiochiometric) oxide-induced surface states. As a result of this direct correlation between growth of native SiOx and high density of surface states, the prevailing strategy in Si electronic passivation by organic monolayers is to increase the molecular coverage of the atop surface Si atoms,[74] which will prevent the growth of SiOx. However, our results clearly show that in terms of electrical passivation per se (regardless of stability) relaxing specific, active sites on the Si surface is the critical action, rather than efficient coverage, as in the case of alkoxy$_{80}$ compared to the alkyl monolayer. The former is less dense and the coverage lower than the latter, but its electronic passivation is superior.

On the basis of this study and the results for the alkoxy$_{UV}$ samples we can suggest a more general observation. It appears that efficient electrical passivation is achieved by *reactivity*-driven binding, while good chemical passivation, at least in terms of dense coverage, results from efficient "*self-assembly*" adsorption. Namely, the binding of one molecule facilitates dense binding in its vicinity due to the extremely short diffusion distance of the free radical on the Si for RCR, or van der Waals attraction of alkyl chains in the general case.[48] Thus for any given surface, one can devise a dual surface treatment, where the substrate is reacted both with a defect-specific reagent and with self-assembling monomers. Naturally, these could be either two different chemical species or one adsorbate under different reaction conditions.

The importance of this finding stems from the critical role of surface states in determining the current−voltage behavior and photovoltaic performance of full Si-monolayer/metal junctions. Although the BB values for the alkoxy$_{80}$ monolayer indicate that its electronic passivation is efficient, its small effect on surface potential and poor long-term stability render it unattractive for making strongly rectifying junctions, as is needed for photovoltaic activity. Therefore, it is not further considered in our discussion of the dark and photocurrent−voltage behavior of the junctions.

Charge Transport (Current−Voltage) in the Dark and Photovoltaic Performance. As mentioned above, passivation is essential for superior device performance, and furthermore, device characteristics are in fact the most sensitive probe of electrical and chemical passivation. Therefore, we turn to examining the manifestation of the above considerations in practical devices.

The current−voltage behavior of junctions that form upon contacting the monolayer-covered Si surfaces with Hg to create n-Si-alkoxy$_{UV}$/Hg and n-Si-alkyl/Hg junctions is presented in Figure 6. It is apparent that both junctions are rectifying and

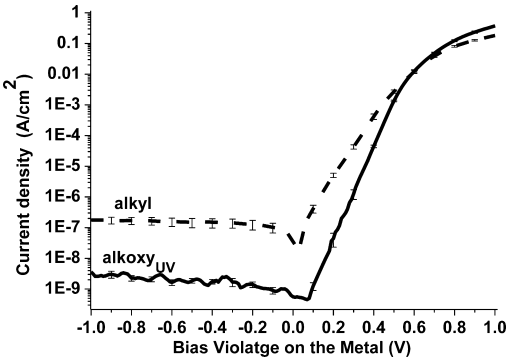

Figure 6. Current−voltage characteristics in the dark of n-Si -monolayer/Hg junctions with alkoxy$_{UV}$ (solid line) and alkyl (dashed line) monolayers. Results are logarithmic averages of at least 15 different junctions on at least 3 samples with a scan rate of 20 mV/s. The error bars represent standard deviations, which are typically <5% of the measured currents.

have semilogarithmic current−voltage dependence at forward bias. However, they differ considerably in the magnitude of the reverse bias and the slope of the semilogarithmic forward bias characteristic.

It has been shown that the n-Si-alkyl/Hg (Figure 6—dashed line) junction is in strong inversion and that transport across it is dominated by minority carriers.[65,71] As discussed previously,[65] the alkyl monolayer enables the formation of such a junction, both because of the large surface dipole that it introduces, which decreases the effective Si electron affinity, and by providing sufficient electronic passivation that prevents Fermi level pinning. As we showed in the previous sections the alkoxy$_{UV}$ monolayer induces an even larger decrease in the Si electron affinity and provides better electronic passivation than the alkyl one. The results presented in Figure 6 indicate that the superior properties of the alkxoy$_{UV}$ monolayer are indeed reflected in the current−voltage behavior.

The critical role of surface passivation is even clearer if we consider the magnitude of the reverse bias currents. To a first approximation the reverse bias current density of a p^+−n junction that includes both diffusion and generation currents is given by[75]

$$J_R = q\sqrt{\frac{D_p}{\tau_p}}\frac{n_i^2}{N_D} + \frac{qn_iW}{\tau_{eff}} \quad (1)$$

dx.doi.org/10.1021/jp4027755 | J. Phys. Chem. C 2013, 117, 22351−22361

where D_p and τ_p are, respectively, the hole diffusion coefficient and lifetime in the Si bulk; n_i is the intrinsic carrier concentration; N_D is the doping density; W is the depletion layer width; and τ_{eff} is the effective minority carrier lifetime in the depletion layer. The first term represents the contribution from diffusion in the bulk, and the second is from generation currents in the depletion layer.

The diffusion term is extremely small for Si, on the order of 10^{-13} A/cm^2, i.e., completely negligible compared to the measured reverse bias current densities (Figure 6). The depletion layer width, W, is the same for both surfaces (alkyl and alkoxy$_{UV}$) because they are both strongly inverted.[76] This leaves τ_{eff} as the only parameter that can account for the considerably lower reverse current for the alkoxy$_{UV}$ than for the alkyl monolayer. Indeed, the lifetime, τ_{eff}, extracted from photoconductivity decay (PCD, see Table 2) measurements, is 4 times larger for junctions with alkoxy$_{UV}$ than for those with alkyl monolayers. We note, however, that to fully explain the observed reduction in reverse current eq 1 suggests that the τ_{eff} value would have to be $\sim 10^2$ times larger for the alkoxy$_{UV}$ junction than for the alkyl one. This apparent inconsistency stems from the dependence of τ_{eff} on the concentration of carriers at the surface,[77,78] with minimal lifetime for a depleted semiconductor and increasing lifetime for accumulation or inversion of the surface.[79] In the contactless PCD measurement, both surfaces are depleted, whereas in the complete device, including the Hg contact, the Si surfaces are both in strong inversion. In that case, due to the larger surface dipole of the alkoxy$_{UV}$ with respect to the alkyl monolayer (cf. Table 2), the Si is more strongly inverted for the alkoxy$_{UV}$ case, emphasizing the superior passivation that it had in the first place.

Because the junction is in strong inversion, it can be interpreted in a manner similar to that for p−n junctions.[75] We consider first the current−voltage curves under forward bias, according to the accepted representation of a diode's forward bias current

$$J_F \propto \exp\left(\frac{qV}{nkT}\right) \quad (2)$$

where q is the electronic charge; kT is the thermal energy; V is the applied bias; and n is the diode "ideality factor". For minority carrier-controlled junctions, i.e., a p−n junction or strongly inverted metal−semiconductor (MS) junction, n = 1 or 2 for current dominated by diffusion or recombination, respectively.

The ideality factor, n, for both junctions, presented in Figure 6, was calculated from the slopes of the semilogarithmic curves over the 0.05−0.55 V bias range. For the alkoxy$_{UV}$ sample (Figure 6, solid curve) n = 1.1 with a very good quality of fit (R^2 = 0.99954), while for the alkyl one (Figure 6, dashed curve), n = 1.6 and the curve deviates noticeably from linearity (R^2 = 0.99542). The increase in n value indicates that recombination of minority carriers at the Si surface is much more significant in the alkyl junction than in the alkoxy$_{UV}$ one. Thus, we see how the superior passivation of the alkoxy$_{UV}$, as expressed in low band bending values and high minority carrier lifetimes (Table 2), is also reflected in the current−voltage characteristics.

To summarize this section, both a lower density of surface states (according to the PCD and CPD measurements) and a larger change in surface potential (according to CPD measurements) contribute to the superior passivation using the alkoxy$_{UV}$ monolayer.

Photovoltaic (PV) Performance. The superior diode behavior of the alkoxy$_{UV}$/Hg junction, compared to that of the alkyl/Hg one (Figure 6), suggests that it will also exhibit superior photovoltaic (PV) performance.[80] In Figure 7 we demonstrate the correlation between the diode behavior of the junction in the dark and under illumination, i.e., its PV performance. Figure 7 presents the PV currents measured for two representative junctions, a Si-alkoxy$_{UV}$/Hg one (solid line) and a Si-alkyl/Hg (dashed line) one, under 561 nm laser illumination. The incident laser was directed under the Hg drop, and its intensity was adjusted to generate a short-circuit current (J_{SC}) of ∼30 mA/cm^2 for the sake of comparison between measurements. Because J_{SC} is adjusted manually, the informative parameter is the open-circuit voltage (V_{OC}) and, to a lesser extent, the fill factor (FF) of the illuminated junction. V_{OC} is the voltage, produced by the junction at zero current, and FF is the ratio between the maximum power, produced by the junction and the product of the V_{OC} and J_{SC}. Both are commonly used measures for PV performance.[15,16]

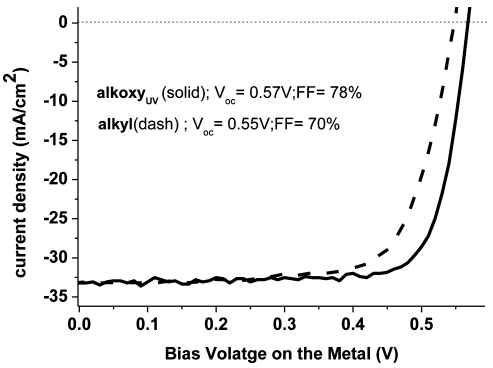

Figure 7. Photovoltaic current−voltage characteristics for the Si-alkoxy$_{UV}$/Hg (solid line) and Si-alkyl/Hg (dashed line) with 561 nm laser illumination, the intensity of which was adjusted to produce a short-circuit current (J_{sc}) ∼ 30 mA/cm^2. V_{oc} and FF values are noted in the figure.

Figure 7 shows that the V_{oc} (and FF) of the alkoxy$_{UV}$ junction are higher than that of the alkyl junction (for the same J_{SC}). The results agree with the lower density of surface states and lower dark reverse currents (negative bias), which are presented in Table 2 and Figure 6, respectively. They demonstrate how the superior electronic passivation of the alkoxy$_{UV}$ monolayer, which stems from the strong preference of the alcohol molecules toward specific electronically active sites on the one hand and from the high coverage (due to the nonsite-specific radical formation) on the other hand, is expressed in charge transport and photovoltaic behavior.

SUMMARY AND CONCLUSIONS

The reaction between 1-alcohols and the H-terminated Si(111) surface can take place through two different reaction mechanisms, namely, nucleophilic substitution, S_N, and radical chain reaction, RCR. This duality in the possible reaction path was used in this study as a tool to explore fundamentals of Si surface passivation by organic monolayers. Combined spectroscopic and computational evidence points to different binding configuration under the different reaction conditions. We find that, because the nucleophilic substitution is site-sensitive, this

type of reaction improves the electrical passivation of the Si surface. The reason is that it passivates selectively the kinks and steps on the Si surface, which are not only chemically reactive but also a major source of surface states. However, because the product of the S_N reaction is a Si−O bond, it is unstable toward, e.g., hydrolysis.[11,33,34] In contrast, the radical chain reaction is fast and not site-specific. The resulting binding configuration of this reaction is Si−CH(OH)−R, which is denser and much less susceptible toward further reactions and is, thus, more stable and provides better chemical passivation.

The benefits of chemical and electrical passivation are combined by reacting R−CH_2−OH at room temperature to promote efficient elimination of surface states by S_N, combined with the UV-initiated radical chain reaction that leads to a dense, chemically stable monolayer. The superior electrical passivation is expressed in a longer lifetime of minority carriers, a more rectifying diode behavior in the dark, and higher open-circuit photovoltage and fill factor under illumination. The presence of OH groups that results from RCR binding of alcohol to the Si surface explains the large difference in surface potential between the alkoxy monolayers that are formed by UV activation and those formed upon moderate (80 °C) heating. The effect of the strong reduction in the WF of Si, combined with efficient electrical passivation achieved with the $alkoxy_{UV}$ monolayer, is illustrated by its improved photovoltaic performance compared to that of the alkyl one.

This study on alcohol binding to Si−H suggests that there is an important and overlooked inherent trade-off between the stability of a monolayer (i.e., chemical passivation) and its electronic passivating action. Efficient chemical passivation is achieved by the formation of chemical bonds with small polarization, such as Si−C, which form a dense monolayer via radical chain reaction. However, because this reaction mechanism is not site-sensitive, the resulting electronic passivation is not efficient. The opposite is the case for the nucleophilic substitution, where the reaction mechanism is site-sensitive (and, thus, results in high electronic passivation), but the resulting bond is polar and, thus, susceptible to further reaction, which makes it chemically unstable.

Our results suggest a way to overcome this apparent contradiction between chemical and electrical passivation, viz., by preparing monolayers where one adsorbate type or condition is selective toward the most reactive sites (e.g., nucleophilic substitution) and by that passivates the electrically active defects and another adsorbate or condition forms densely packed monolayers with a stable bond (e.g., radical chain reactions). This monolayer effectively prevents surface oxidation within detectable levels. We suggest that elimination of (reactive) surface states by a site-specific reaction may be especially important for surfaces which are more prone to defects such as those of dihydride-terminated (100) Si−H (compared to the monohydride-terminated (111) Si−H one) and, likely, also for surfaces of other semiconductors.

■ ASSOCIATED CONTENT

Ⓢ Supporting Information

OH signal in a FT-IR spectra of the Si-$alkoxy_{UV}$. This material is available free of charge via the Internet at http://pubs.acs.org.

■ AUTHOR INFORMATION

Corresponding Author

*David Cahen. Tel.: 972-8-934-2246. E-mail: david.cahen@weizmann.ac.il. Ayelet Vilan. Tel.: 972-8-934-3729. E-mail: ayelet.vilan@weizmann.ac.il. Leeor Kronik. Tel.: 972-8-934-4993. E-mail: leeor.kronik@weizmann.ac.il.

Notes

The authors declare no competing financial interest.

■ ACKNOWLEDGMENTS

We thank Ofer Sinai, Ariel Biller, Pabitra Kumar Nayak (WIS), Chaim Sukenik (Bar-Ilan), J. Schwartz (Princeton), and Yves Chabal (UT Dallas) for useful discussions and guidance. A.V., L.K., and D.C. thank the Israel Science Foundation via its centres of Excellence program, for partial support. D.C. & L.K. thank the Wolfson family trust and the Leona M. and Harry B. Helmsley Charitable Trust, and D.C. thanks the Grand Centre for Sensors and Security and the Kimmel Centre for Nanoscale Science for support. L.K. thanks the Lise Meitner Minerva Center for Computational Chemistry. D.A.E. is a recipient of a DOC-fellowship by the Austrian Academy of Sciences, and further financial support by the Austrian Science Fund (FWF): I937-N19 is gratefully acknowledged. O.Y. thanks the Azrieli Foundation for the award of an Azrieli Fellowship. D.C. holds the Rowland and Sylvia Schaefer chair in Energy research.

■ REFERENCES

(1) Li, Y.; Calder, S.; Yaffe, O.; Cahen, D.; Haick, H.; Kronik, L.; Zuilhof, H. Hybrids of Organic Molecules and Flat, Oxide-Free Silicon: High-Density Monolayers, Electronic Properties, And Functionalization. *Langmuir* **2012**, *28*, 9920−9.

(2) Vilan, A.; Yaffe, O.; Biller, A.; Salomon, A.; Kahn, A.; Cahen, D. Molecules on Si: Electronics with Chemistry. *Adv. Mater.* **2010**, *22*, 140−59.

(3) Cohen, Y. S.; Vilan, A.; Ron, I.; Cahen, D. Hydrolysis Improves Packing Density of Bromine-Terminated Alkyl-Chain, Silicon−Carbon Monolayers Linked to Silicon. *J. Phys. Chem. C* **2009**, *113*, 6174−6181.

(4) Anagaw, A. Y.; Wolkow, R. A.; DiLabio, G. A. Theoretical Study of Work Function Modification by Organic Molecule-Derived Linear Nanostructure on H-Silicon(100)-2 × 1. *J. Phys. Chem. C* **2008**, *112*, 3780−3784.

(5) Hartig, P.; Dittrich, T.; Rappich, J. Surface Dipole Formation and Non-Radiative Recombination at p-Si(111) Surfaces during Electrochemical Deposition of Organic Layers. *J. Electroanal. Chem.* **2002**, *524*−*525*, 120−126.

(6) Rappich, J.; Merson, A.; Roodenko, K.; Dittrich, T.; Gensch, M.; Hinrichs, K.; Shapira, Y. Electronic Properties of Si Surfaces and Side Reactions during Electrochemical Grafting of Phenyl Layers. *J. Phys. Chem. B* **2006**, *110*, 1332−7.

(7) Hacker, C. A. Solid-State Electronics Modifying Electronic Properties at the Silicon − Molecule Interface Using Atomic Tethers. *Solid-State Electron.* **2010**, *54*, 1657−1664.

(8) Hunger, R.; Jaegermann, W.; Merson, A.; Shapira, Y.; Pettenkofer, C.; Rappich, J. Electronic Structure of Methoxy-, Bromo-, and Nitrobenzene Grafted onto Si(111). *J. Phys. Chem. B* **2006**, *110*, 15432−41.

(9) Magid, I.; Burstein, L.; Seitz, O.; Segev, L.; Kronik, L.; Rosenwaks, Y. Electronic Characterization of Si(100)-Bound Alkyl Monolayers Using Kelvin Probe Force Microscopy. *J. Phys. Chem. C* **2008**, *112*, 7145−7150.

(10) Natan, A.; Zidon, Y.; Shapira, Y.; Kronik, L. Cooperative Effects and Dipole Formation at Semiconductor and Self-Assembled-Monolayer Interfaces. *Phys. Rev. B* **2006**, *73*, 193310.

(11) Faber, E. J.; De Smet, L. C. P. M.; Olthuis, W.; Zuilhof, H.; Sudhölter, E. J. R.; Bergveld, P.; Van den Berg, A. Si-C Linked Organic Monolayers on Crystalline Silicon Surfaces As Alternative Gate Insulators. *Chem. Phys. Phys. Chem.* **2005**, *6*, 2153−66.

(12) Webb, L. J.; Lewis, N. S. Comparison of the Electrical Properties and Chemical Stability of Crystalline Silicon(111) Surfaces Alkylated

Using Grignard Reagents or Olefins with Lewis Acid Catalysts. *J. Phys. Chem. B* **2003**, *107*, 5404−5412.
(13) Sieval, A. B.; Huisman, C. L.; Schönecker, A.; Schuurmans, F. M.; Van der Heide, A. S. H.; Goossens, A.; Sinke, W. C.; Zuilhof, H.; Sudhölter, E. J. R. Silicon Surface Passivation by Organic Monolayers: Minority Charge Carrier Lifetime Measurements and Kelvin Probe Investigations. *J. Phys. Chem. B* **2003**, *107*, 6846−6852.
(14) Zhao, J.; Uosaki, K. Dielectric Properties of Organic Monolayers Directly Bonded on Silicon Probed by Current Sensing Atomic Force Microscope. *Appl. Phys. Lett.* **2003**, *83*, 2034.
(15) Fonash, S. *Solar Cell Device Physics*, 2nd ed.; Academic Press: New York, 2010.
(16) Nelson, J. *The Physics of Solar Cells (Properties of Semiconductor Materials)*; Imperial College Press: U.K., 2003.
(17) Scheres, L.; Arafat, A.; Zuilhof, H. Self-Assembly of High-Quality Covalently Bound Organic Monolayers onto Silicon. *Langmuir* **2007**, *23*, 8343−6.
(18) Puniredd, S. R.; Assad, O.; Haick, H. Highly Stable Organic Monolayers for Reacting Silicon with Further Functionalities: The Effect of the C−C Bond Nearest the Silicon Surface. *J. Am. Chem. Soc.* **2008**, *130*, 13727−34.
(19) Boukherroub, R.; Morin, S.; Sharpe, P.; Wayner, D. D. M.; Allongue, P. Insights into the Formation Mechanisms of Si−OR Monolayers from the Thermal Reactions of Alcohols and Aldehydes with Si(111)−H 1. *Langmuir* **2000**, *16*, 7429−7434.
(20) Ciampi, S.; Harper, J. B.; Gooding, J. J. Wet Chemical Routes to the Assembly of Organic Monolayers on Silicon Surfaces via the Formation of Si−C Bonds: Surface Preparation, Passivation and Functionalization. *Chem. Soc. Rev.* **2010**, *39*, 2158−83.
(21) Newton, T. A.; Lepak, L. A.; Hines, M. A. The Site-Specific Reactivity of Isopropanol in Aqueous Silicon Etching: Controlling Morphology with Surface Chemistry. *Chem. Phys.* **1999**, *111*, 20−23.
(22) Cohen, R.; Zenou, N.; Cahen, D.; Yitzchaik, S. Molecular Electronic Tuning of Si Surfaces. *Chem. Phys. Lett* **1997**, *279*, 270−274.
(23) Salomon, A.; Böcking, T.; Gooding, J. J.; Cahen, D. How Important Is the Interfacial Chemical Bond for Electron Transport through Alkyl Chain Monolayers? *Nano Lett.* **2006**, *6*, 2873−6.
(24) Nesher, G.; Shpaisman, H.; Cahen, D. Effect of Chemical Bond Type on Electron Transport in GaAs-Chemical Bond-Alkyl/Hg Junctions. *J. Am. Chem. Soc.* **2007**, *129*, 734−5.
(25) Thieblemont, F.; Seitz, O.; Vilan, A.; Cohen, H.; Salomon, E.; Kahn, A.; Cahen, D. Electronic Current Transport through Molecular Monolayers: Comparison between Hg/Alkoxy and Alkyl Monolayer/Si(100) Junctions. *Adv. Mater.* **2008**, *20*, 3931−3936.
(26) Corriu, R. J. P.; Guerin, C. Nucleophilic Displacement at Silicon: Recent Developments and Mechanistic Implications. *Adv. Organomet. Chem.* **1982**, *20*, 265−312.
(27) Chatgilialoglu, C. *Organosilanes in Radical Chemistry*; John Wiley & Sons: New York, 2004; p 240.
(28) Holmes, R. R. The Stereochemistry of Nucleophilic Substitution of Tetracoordinate Silicon. *Chem. Rev.* **1990**, *90*, 17−31.
(29) Kharasch, M. S.; Rowe, J. L.; Urry, W. H. Reactions of Atoms and Free Radicals in Solution. XXVII. The Decomposition of Diacetyl Peroxide in Alcohols. *J. Org. Chem.* **1951**, *16*, 905−913.
(30) Urry, W. H.; Stacey, F. W.; Huyser, E. S.; Juveland, O. O. The Peroxide- and Light-Induced Additions of Alcohols to Olefins. *J. Am. Chem. Soc.* **1954**, *76*, 450−455.
(31) Liu, Z.-Q.; Sun, L.; Wang, J.-G.; Han, J.; Zhao, Y.-K.; Zhou, B. Free-Radical-Initiated Coupling Reaction of Alcohols and Alkynes: Not C−O but C−C Bond Formation. *Org. Lett.* **2009**, *11*, 1437−9.
(32) Tzirakis, M. D.; Alberti, M. N.; Orfanopoulos, M. Hydroxyalkylation of [60]Fullerene: Free Radical Addition of Alcohols to C60. *Chem. Commun.* **2010**, *46*, 8228−30.
(33) Linford, M. R.; Fenter, P.; Eisenberger, P. M.; Chidsey, C. E. D. Alkyl Monolayers on Silicon Prepared from 1-Alkenes and Hydrogen-Terminated Silicon. *J. Am. Chem. Soc.* **1995**, *117*, 3145−3155.
(34) Calistri-Yeh, M.; Kramer, E. J.; Sharma, R.; Zhao, W.; Rafailovich, M. H.; Sokolov, J.; Brock, J. D. Thermal Stability of Self-Assembled Monolayers from Alkylchlorosilanes. *Langmuir* **1996**, *12*, 2747−2755.
(35) Higashi, G. S.; Chabal, Y. J.; Trucks, G. W.; Raghavachari, K. Ideal Hydrogen Termination of the Si(111) Surface. *Appl. Phys. Lett.* **1990**, *56*, 656.
(36) Higashi, G. S.; Becker, R. S.; Chabal, Y. J.; Becker, A. J. Comparison of Si(111) Surfaces Prepared Using Aqueous Solutions of NH4F versus HF. *Appl. Phys. Lett.* **1991**, *58*, 1656.
(37) Hines, M. A.; Chabal, Y. J.; Harris, T. D.; Harris, A. L. Measuring the Structure of Etched Silicon Surfaces with Raman Spectroscopy. *Structure* **1994**, 07974.
(38) Reider, G.; Höfer, U.; Heinz, T. Surface Diffusion of Hydrogen on Si(111)7 × 7. *Phys. Rev. Lett.* **1991**, *66*, 1994−1997.
(39) Eves, B. J.; Sun, Q.-Y.; Lopinski, G. P.; Zuilhof, H. Photochemical Attachment of Organic Monolayers onto H-Terminated Si(111): Radical Chain Propagation Observed via STM Studies. *J. Am. Chem. Soc.* **2004**, *126*, 14318−9.
(40) Buriak, J. M. Organometallic Chemistry on Silicon and Germanium Surfaces. *Chem. Rev.* **2002**, *102*, 1271−1308.
(41) Linford, M. R.; Fenter, P.; Eisenberger, P. M.; Chidsey, C. E. D. Alkyl Monolayers on Silicon Prepared from 1-Alkenes and Hydrogen-Terminated Silicon. *J. Am. Chem. Soc.* **1995**, *117*, 3145−3155.
(42) Salomon, A.; Boecking, T.; Chan, C.; Amy, F.; Girshevitz, O.; Cahen, D.; Kahn, A. How Do Electronic Carriers Cross Si-Bound Alkyl Monolayers? *Phys. Rev. Lett.* **2005**, *95*, 1−4.
(43) Seitz, O.; Böcking, T.; Salomon, A.; Gooding, J. J.; Cahen, D. Importance of Monolayer Quality for Interpreting Current Transport through Organic Molecules: Alkyls on Oxide-Free Si. *Langmuir* **2006**, *22*, 6915−22.
(44) Wallart, X.; Villeneuve, C. H. De; Allongue, P. Truly Quantitative XPS Characterization of Organic Monolayers on Silicon: Study of Alkyl and Alkoxy Monolayers on H-Si (111). *Langmuir* **2005**, 7871−7878.
(45) Sieval, A. B.; Van den Hout, B.; Zuilhof, H.; Sudhölter, E. J. R. Molecular Modeling of Alkyl Monolayers on the Si(111) Surface. *Langmuir* **2000**, *16*, 2987−2990.
(46) Ahrenkiel, R. K.; Johnston, S. Contactless Measurement of Recombination Lifetime in Photovoltaic Materials. *Sol. Energy Mater. Sol. Cells* **1998**, *55*, 59−73.
(47) Segev, L.; Salomon, A.; Natan, A.; Cahen, D.; Kronik, L.; Amy, F.; Chan, C.; Kahn, A. Electronic Structure of Si(111)-Bound Alkyl Monolayers: Theory and Experiment. *Phys. Rev. B* **2006**, *74*, 1−6.
(48) Bent, S. F. Heads or Tails: Which Is More Important in Molecular Self-Assembly? *ACS Nano* **2007**, *1*, 10−2.
(49) Perdew, J. P.; Burke, K.; Ernzerhof, M. Generalized Gradient Approximation Made Simple. *Phys. Rev. Lett.* **1996**, *77*, 3865−3868.
(50) Kresse, G. Efficient Iterative Schemes for Ab Initio Total-Energy Calculations Using a Plane-Wave Basis Set. *Phys. Rev. B* **1996**, *54*, 11169−11186.
(51) Makov, G.; Payne, M. Periodic Boundary Conditions in Ab Initio Calculations. *Phys. Rev. B* **1995**, *51*, 4014−4022.
(52) Natan, A.; Kronik, L.; Shapira, Y. Computing Surface Dipoles and Potentials of Self-Assembled Monolayers from First Principles. *Appl. Surf. Sci.* **2006**, *252*, 7608−7613.
(53) Neugebauer, J.; Scheffler, M. Adsorbate−Substrate and Adsorbate−Adsorbate Interactions of Na and K Adlayers on Al(111). *Phys. Rev. B* **1992**, *46*, 16067−16080.
(54) Köhler, L.; Kresse, G. Density Functional Study of CO on Rh(111). *Phys. Rev. B* **2004**, *70*, 165405.
(55) Aqua, T.; Cohen, H.; Sinai, O.; Frydman, V.; Bendikov, T.; Krepel, D.; Hod, O.; Kronik, L.; Naaman, R. Role of Backbone Charge Rearrangement in the Bond-Dipole and Work Function of Molecular Monolayers. *J. Phys. Chem. C* **2011**, *115*, 24888−24892.
(56) Porter, M. D.; Bright, T. B.; Allara, D. L.; Chidsey, C. E. D. Spontaneously Organized Molecular Assemblies. 4. Structural Characterization of n-Alkyl Thiol Monolayers on Gold by Optical Ellipsometry, Infrared Spectroscopy, And Electrochemistry. *J. Am. Chem. Soc.* **1987**, *109*, 3559−3568.

(57) Snyder, R. G.; Strauss, H. L.; Elliger, C. A. Carbon-Hydrogen Stretching Modes and the Structure of n-Alkyl Chains. 1. Long, Disordered Chains. *J. Phys. Chem.* **1982**, *86*, 5145−5150.
(58) Values of 2915−2920 cm^{-1} are typical for densely packed alkanes, and 2926−2928 cm^{-1} values characterize liquid alkenes.
(59) Lin-Vien, D.; Colthup, N. B.; Fateley, W. G.; Grasselli, J. G. *The Handbook of Infrared and Raman Characteristic Frequencies of Organic Molecules*; Academic Press: New York, 1991.
(60) Wen, K.; Maoz, R.; Cohen, H.; Sagiv, J.; Gibaud, A.; Desert, A.; Ocko, B. M. Postassembly Chemical Modification of a Highly Ordered Organosilane Multilayer: New Insights into the Structure, Bonding, And Dynamics of Self-Assembling Silane Monolayers. *ACS Nano* **2008**, *2*, 579−99.
(61) Chabal, Y. UT Dallas, private communication.
(62) Hunger, R.; Fritsche, R.; Jaeckel, B.; Jaegermann, W.; Webb, L.; Lewis, N. Chemical and Electronic Characterization of Methyl-Terminated Si(111) Surfaces by High-Resolution Synchrotron Photoelectron Spectroscopy. *Phys. Rev. B* **2005**, *72*, 1−7.
(63) Miura, T.; Niwano, M.; Shoji, D.; Miyamoto, N. Kinetics of Oxidation on Hydrogen-Terminated Si(100) and (111) Surfaces Stored in Air. *J. Appl. Phys.* **1996**, *79*, 4373.
(64) Sano, H.; Maeda, H.; Ichii, T.; Murase, K.; Noda, K.; Matsushige, K.; Sugimura, H. Alkyl and Alkoxyl Monolayers Directly Attached to Silicon: Chemical Durability in Aqueous Solutions. *Langmuir* **2009**, *25*, 5516−25.
(65) Yaffe, O.; Scheres, L.; Puniredd, S. R.; Stein, N.; Biller, A.; Lavan, R. H.; Shpaisman, H.; Zuilhof, H.; Haick, H.; Cahen, D.; Vilan, A. Molecular Electronics at Metal/Semiconductor Junctions. Si Inversion by Sub-Nanometer Molecular Films. *Nano Lett.* **2009**, *9*, 2390−4.
(66) Bruening, M.; Cohen, R.; Guillemoles, J. F.; Moav, T.; Libman, J.; Shanzer, A.; Cahen, D. Simultaneous Control of Surface Potential and Wetting of Solids with Chemisorbed Multifunctional Ligands. *J. Am. Chem. Soc.* **1997**, *119*, 5720−5728.
(67) Natan, A.; Kronik, L.; Haick, H.; Tung, R. T. Electrostatic Properties of Ideal and Non-ideal Polar Organic Monolayers: Implications for Electronic Devices. *Adv. Mater.* **2007**, *19*, 4103−4117.
(68) Haick, H.; Ambrico, M.; Ligonzo, T.; Tung, R. T.; Cahen, D. Controlling Semiconductor/Metal Junction Barriers by Incomplete, Nonideal Molecular Monolayers. *J. Am. Chem. Soc.* **2006**, *128*, 6854−69.
(69) Aphek, O. B.; Kronik, L.; Leibovitch, M.; Shapira, Y. Quantitative Assessment of the Photosaturation Technique. *Surf. Sci.* **1998**, *409*, 485−500.
(70) Kronik, L.; Shapira, Y. Surface Photovoltage Phenomena: Theory, Experiment, And Applications. *Surf. Sci. Rep.* **1999**, *37*, 1−206.
(71) Yaffe, O.; Scheres, L.; Segev, L.; Biller, A.; Ron, I.; Salomon, E.; Giesbers, M.; Kahn, A.; Kronik, L.; Zuilhof, H.; Vilan, A.; Cahen, D. Hg/Molecular Monolayer−Si Junctions: Electrical Interplay between Monolayer Properties and Semiconductor Doping Density. *J. Phys. Chem. C* **2010**, *114*, 10270−10279.
(72) Schlüter, M.; Ho, K.; Cohen, M. Step-Dependent Surface States on Silicon(111). *Phys. Rev. B* **1976**, *14*, 550−555.
(73) Nishida, M. On Interpretation of Intrinsic Surface States on the Si(111) Surface. *Phys. Lett. A* **1977**, *63*, 128−130.
(74) Scheres, L.; Giesbers, M.; Zuilhof, H. Self-Assembly of Organic Monolayers onto Hydrogen-Terminated Silicon: 1-Alkynes Are Better than 1-Alkenes. *Langmuir* **2010**, *26*, 10924−9.
(75) Sze, S. M.; Ng, K. K. *Physics of Semiconductor Devices*; Wiley-Interscience: New York, 2006.
(76) Green, M.; King, F.; Shewchun, J. Minority Carrier MIS Tunnel Diodes and Their Application to Electron- And Photo-Voltaic Energy Conversion—I. Theory. *Solid-State Electron.* **1974**, *17*, 551−561.
(77) Shockley, W.; Read, W. Statistics of the Recombinations of Holes and Electrons. *Phys. Rev.* **1952**, *87*, 835−842.
(78) Hall, R. Electron-Hole Recombination in Germanium. *Phys. Rev.* **1952**, *87*, 387−387.
(79) Aberle, A. G.; Glunz, S.; Warta, W. Impact of Illumination Level and Oxide Parameters on Shockley−Read−Hall Recombination at the Si−SiO_2 Interface. *J. Appl. Phys.* **1992**, *71*, 4422.
(80) Har-Lavan, R.; Yaffe, O.; Joshi, P.; Kazaz, R.; Cohen, H.; Cahen, D. Ambient Organic Molecular Passivation of Si Yields Near-Ideal, Schottky−Mott Limited, Junctions. *AIP Adv.* **2012**, *2*, 012164.